# Facile means for quantifying microRNA expression by real-time PCR

Rui Shi and Vincent L. Chiang
*North Carolina State University, Raleigh, NC, USA*

*BioTechniques 39:519-525 (October 2005)*
*doi 10.2144/000112010*

*MicroRNAs (miRNAs) are 20–24 nucleotide RNAs that are predicted to play regulatory roles in animals and plants. Here we report a simple and sensitive real-time PCR method for quantifying the expression of plant miRNAs. Total RNA, including miRNAs, was polyadenylated and reverse-transcribed with a poly(T) adapter into cDNAs for real-time PCR using the miRNA-specific forward primer and the sequence complementary to the poly(T) adapter as the reverse primer. Several* Arabidopsis *miRNA sequences were tested using SYBR® Green reagent, demonstrating that this method, using as little as 100 pg total RNA, could readily discriminate the expression of miRNAs having as few as one nucleotide sequence difference. This method also revealed miRNA tissue-specific expression patterns that cannot be resolved by Northern blot analysis and may therefore be widely useful for characterizing miRNA expression in plants as well as in animals.*

## INTRODUCTION

MicroRNAs (miRNAs) are released from long hairpin-containing miRNA precursors (pre-miRNAs) as 20–24 nucleotide single-stranded mature miRNAs and enter and guide the RNA-induced silencing complex (RISC) to identify target messages for silencing through either direct mRNA cleavage or translational repression (for recent reviews, see References 1 and 2). Such miRNA-mediated gene silencing has been predicted to regulate various developmental, metabolic, and cellular processes (1,2). Thus, the spatiotemporal expression patterns of miRNAs are important to the verification of their predicted functions. Northern blot analysis, the principal technique for detecting RNA transcripts, is however often insensitive for miRNAs (3,4). As miRNA identification efforts have been shifted from cloning to computation (5–8), a more sensitive and high-throughput method for quantifying the expression of a large number of in silico miRNAs is needed for verifying their authenticity and functions.

In addition to Northern blot analysis, many miRNA detection systems have recently been developed, such as *mir*Vana™ miRNA Detection (Ambion, Austin, TX, USA), the invader assay-based detection (9), *mir*MASA™ miRNA profiling (Genaco Biomedical Products, Huntsville, AL, USA) (10), and modified microarrays (11–16). All these hybridization-based methods require large quantities of RNA. A more sensitive real-time PCR method has been developed for quantifying the expression of pre-miRNAs (17). However, this method cannot detect mature miRNAs. Here we report the establishment and validation of a simple, high-throughput real-time PCR method for quantifying plant miRNAs based on techniques and materials readily available to the general scientific community.

## MATERIALS AND METHODS

### RNA Isolation, Polyadenylation, and Reverse Transcription

Total RNA was isolated from leaf and stem tissues of *Arabidopsis thaliana* (Columbia accession) using TRIZOL® reagent (Invitrogen, Carlsbad, CA, USA) and treated with RNase-free DNaseI (Promega, Madison, WI, USA). The treated total RNA (1 µg) was polyadenylated with ATP by poly(A) polymerase (PAP) at 37°C for 1 h in a 20-µL reaction mixture following the manufacturer's directions for the Poly(A) Tailing Kit (Ambion). After phenol-chloroform extraction and ethanol precipitation, the RNAs were dissolved in diethylpyrocarbonate (DEPC)-treated water and reverse-transcribed with 200 U SuperScript™ II Reverse Transcriptase (Invitrogen) and 0.5 µg poly(T) adapter [3′ rapid amplification of complementary DNA ends (RACE) adapter in the FirstChoice® RLM-RACE kit; Ambion] according to the manufacturer's protocols (Invitrogen).

### Real-Time PCR Primer Design and Melting Temperature Evaluation

Seven miRNAs were selected, covering a variety of miRNA sequence features. AthmiR159a and AthmiR161 each represent the single member in the corresponding miRNA families (3,18). AthmiR165a and AthmiR166a differ by 1 nucleotide (3), and AthmiR167a (3) and its two paralogues, AthmiR167c and AthmiR167d, have 1 to 2 nucleotide differences (5,18). AthmiR159a, AthmiR165a, and AthmiR166a are each located at the 3′ arm of their cognate pre-miRNAs, whereas all the other tested miRNAs are on the 5′ arm of the corresponding pre-miRNAs. *Arabidopsis* 5.8S ribosomal RNA (rRNA) was selected as the internal reference gene for PCR quantitation. The reverse primer for these miRNAs and 5.8S rRNA was a 3′ adapter primer (3′ RACE outer primer in the FirstChoice RLM-RACE kit), and the forward primer was designed based on the entire tested miRNA sequence. However, for those forward primers containing more than three G/C within the five 3′-end nucleotides, one or two As were added to the 3′ end of these primers to ensure their binding to the target site encompassing the miRNA sequence and Ts in the poly(T) adapter (Figure 1). For 5.8S rRNA, the forward primer contained sequences complementary to those located at the 3′ end. These primer designs were expected to result in 63–65 bp products. All primers used in this study were synthesized by MWG Biotech (Highpoint, NC, USA) and are listed in Table 1.

**Table 1. Primers Used in the Study**

| Name | Sequence |
|---|---|
| AthmiR159a | 5′-TTTGGATTGAAGGGAGCTCTA-3′ |
| AthmiR159a anti | 5′-TAGAGCTCCCTTCAATCCAAA-3′ |
| AthmiR161 | 5′-GAAAGTGACTACATCGGGGAA-3′ |
| AthmiR161 anti | 5′-CCCCGATGTAGTCACTTTCAA-3′ |
| AthmiR165a | 5′-CGGACCAGGCTTCATCCC-3′ |
| AthmiR166a | 5′-CGGACCAGGCTTCATTCC -3′ |
| AthmiR166–3m | 5′-CGGACCTCCCTTCATTCC-3′ |
| AthmiR166–2m | 5′-CGGACCTGGCTTCTTTCC-3′ |
| AthmiR166-m1 | 5′-CGCACCAGGCTTCATTCC-3′ |
| AthmiR166-m2 | 5′-CGGTCCAGGCTTCATTCC-3′ |
| AthmiR166-m3 | 5′-CGGACCAGGCTTGATTCC-3′ |
| AthmiR166 anti | 5′-GGGAATGAAGCCTGGTCCGA-3′ |
| AthmiR167a | 5′-TGAAGCTGCCAGCATGATCTA-3′ |
| AthmiR167c | 5′-TTAAGCTGCCAGCATGATCTT-3′ |
| AthmiR167d | 5′-TGAAGCTGCCAGCATGATCTGG-3′ |
| AthmiR167a anti | 5′-TAGATCATGCTGGCAGCTTCA-3′ |
| Ath5.8S | 5′-ACGTCTGCCTGGGTGTCACAA-3′ |
| Poly(T) adapter | 5′-GCGAGCACAGAATTAATACGACTCACTATAGG(T)12VN*-3′ |
| Reverse primer | 5′-GCGAGCACAGAATTAATACGAC-3′ |

*V = A, G, C; N = A, T, G, C.

The true melting temperature ($T_m$) values of primers were experimentally determined from the thermal dissociation curves generated from the target primers and their corresponding antisense sequences using an ABI PRISM® 7000HT Sequence Detection System (Applied Biosystems, Foster City, CA, USA). Briefly, 100 pmol each of the primer and its antisense oligonucleotide were mixed with 12.5 µL SYBR® Green PCR Master Mix (Applied Biosystems) in a total volume of 25 µL for DNA melting analysis with a programmed temperature ramp from 45° to 95°C in 5 min to produce a dissociation curve, from which the $T_m$ was calculated.

### Real-Time PCR Amplification of miRNAs and Northern Blot Analysis of miRNA Expression

For each PCR, 1 µL template cDNA, equivalent to approximately 100 pg total RNA, was mixed with 12.5 µL 2× SYBR Green PCR master mix and 5 pmol each of the forward and reverse primers in a final volume of 25 µL. Two amplification programs were used. One was the standard protocol of the ABI PRISM 7000HT Sequence Detection System, 15 s at 95°C and 1 min at 60°C for 45 cycles, and followed by the thermal denaturing step to generate the dissociation curves to verify amplification specificity. This standard PCR protocol was used for quantifying transcript levels of miRNAs differing by two or more nucleotide sequences. The second or modified protocol was 15 s at 95°C, 15 s at a temperature 5°C below the primer's true $T_m$, and 20 s at 72°C for 45 cycles and followed by the thermal denaturing step described above. This high-stringency amplification was designed for quantifying transcript levels of miRNAs with 1 nucleotide difference. All reactions were run in triplicate. PCR product sizes were validated by electrophoresis using 2% agarose or 12% polyacrylamide, 8 M urea gel. Northern blot analysis of miRNA expression was performed according to Lu et al. (19) and Park et al. (20).

### Data Analysis for Real-Time PCR Amplification Efficiency and for Quantifying Relative miRNA Expression

Amplification efficiency of real-time PCR was analyzed according to the protocols of Schmittgen et al. (17). Briefly, a 10-fold dilution series of either cDNA containing the tested miRNA or the purified product of the tested miRNA were used as the template for real-time PCR to generate a plot of log copy numbers of the tested miRNA at different dilutions versus the corresponding cycle threshold ($C_T$). The slope of the linear plot is defined as -(1/log E), where E is the amplification efficiency, and its value should approach 2 if the efficiency reaches the maximum (21). Thus, the quantity of miRNA, relative to a reference gene, can be calculated using the formula $2^{-\Delta CT}$, where $\Delta CT = (C_{T\ miRNA} - C_{T\ reference\ RNA})$ (17). Comparison of miRNA expression was based on a comparative $C_T$ method ($\Delta\Delta C_T$) (21,22), and the relative miRNA expression can be quantified according to the formula of $2^{-\Delta\Delta CT}$, where $\Delta\Delta C_T = (C_{T\ miRNA} - C_{T\ reference\ RNA}) - (C_{T\ calibrator} - C_{T\ reference\ RNA})$ (21,22). The miRNA sample with the lowest $C_T$ value, and thus the highest expression level, was selected as the calibrator, of which expression level represents 100% for normalization in each comparison.

**Table 2. Amplification Efficiency for *Arabidopsis* miRNAs and 5.8S rRNA**

| RNA | PCR Efficiency | $R^2$ |
|---|---|---|
| AtmiR159a | 1.98 | 1 |
| AtmiR161 | 1.99 | 0.9998 |
| AtmiR166a | 1.93 | 0.9985 |
| AtmiR167a | 1.99 | 0.9965 |
| 5.8S rRNA | 1.99 | 0.9968 |

The efficiency test for each microRNA (miRNA) was conducted using total leaf RNA in a range from 1 to 1000 pg.

## RESULTS AND DISCUSSION

Using *Arabidopsis* miRNAs and SYBR Green reagent as a working model, we demonstrated the quantitation of plant miRNA expression through a poly(A) miRNA-based real-time PCR approach (Figure 1). Northern blot analysis of the poly(A) reaction products indicated that the tested miRNAs and 5.8S rRNA could be quantitatively polyadenylated (see Supplementary Figure S1, which can be

found online at www.BioTechniques.com). The dissociation curve showing a unique peak from the PCR amplification of each tested miRNA, as well as 5.8S rRNA, attested to the specificity of the amplification (Figure 2A showing 3 tested miRNAs), while the correct product sizes of 63–65 bp were verified by gel electrophoresis (Figure 2B). The amplification specificity shown by the dissociation curves and gel electrophoresis also provides direct evidence for the exclusion of amplifying the pre-miRNAs by this PCR approach. This is especially true for miRNAs residing on the 5′ arm of their pre-miRNAs, but might not be the case for those located at the 3′ arm, such as AthmiR159a. However, it is well-known that pre-miRNAs have not been compellingly detected in plants (1); not even in plants that are deficient in DCL function (1,3). Using Northern blot analysis, we also could not detect pre-miRNAs of the tested miRNAs. Furthermore, polyadenylation of pre-miRNA might not be efficient due to the presence of the stem-loop structure (23). Taken together, therefore, our PCR approach would be more mature miRNA-specific. Indeed, we failed to amplify the pre-miRNA of AthmiR159a using its pre-miRNA-specific forward primer and poly(T) adaptor reverse primer. This was implicated, based on the $C_T$ values, that in every 100 copies of the products, 99.99 of them were found derived from the mature AthmiR159a (see Supplementary Table S1, which can be found online at www.BioTechniques.com). Thus, the negligible level and low poly(A) efficiency of pre-miRNAs would unlikely affect miRNA quantitation by our real-time PCR approach.

The analysis of PCR results further showed that the amplification efficiency

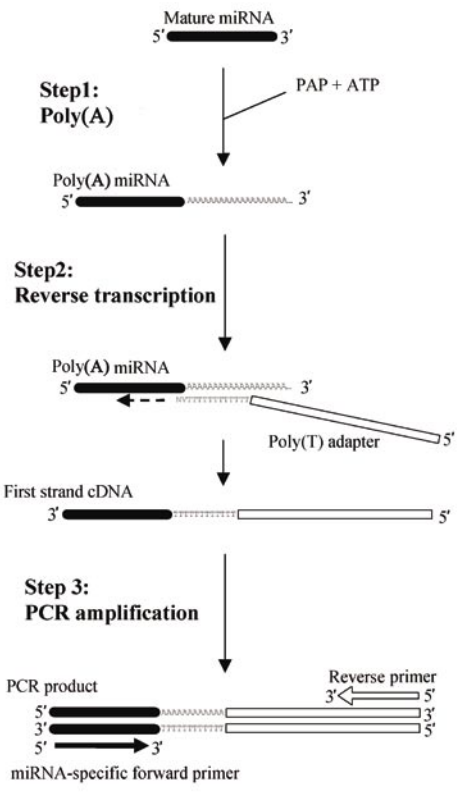


**Figure 1. Real-time PCR quantitation of microRNAs (miRNAs).** Step 1, poly(A) of total RNA to give poly(A) miRNAs. Step 2, reverse transcription of poly(A) miRNAs using poly(T) adapter. Step 3, first strand cDNAs of miRNAs for real-time PCR, with miRNA-specific forward primer and reverse primer complementary to poly(T) adapter. PAP, poly(A) polymerase.

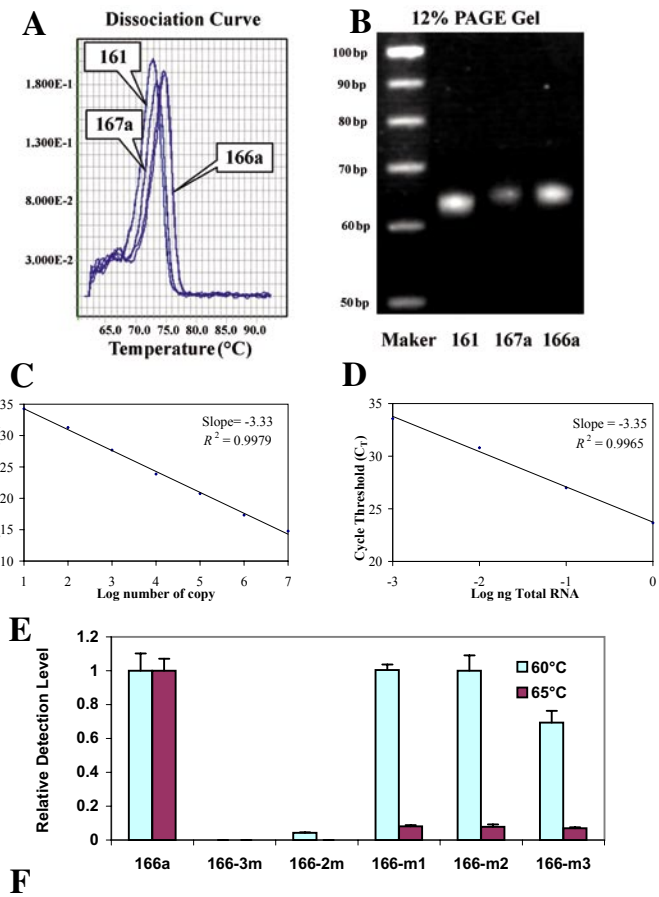


F

| Primer | Sequence | $T_m$* (°C) |
|---|---|---|
| AthmiR166a | 5′-cggaccaggcttcattcc-3′ | 70 |
| AthmiR166-3m | 5′-cggacc**TCC**cttcattcc-3′ | 50 |
| AthmiR166-2m | 5′-cggacc**T**ggcttc**T**ttcc-3′ | 57 |
| AthmiR166-m1 | 5′-cg**C**accaggcttcattcc-3′ | 64 |
| AthmiR166-m2 | 5′-cgg**T**ccaggcttcattcc-3′ | 64 |
| AthmiR166-m3 | 5′-cggaccaggctt**G**attcc-3′ | 63 |

**Figure 2. Validation of real-time PCR for quantitation of microRNAs (miRNAs).** (A) Dissociation curves of real-time PCR amplification of AthmiR161, AthmiR166a, and AthmiR167a. (B) Real-time PCR products with sizes of 63, 64, and 64 bp for AthmiR159a, AthmiR166a, and AthmiR167a, respectively, resolved on ethidium bromide-stained 12% polyacrylamide, 8 M urea gel. (C). Real-time PCR standard curve of diluted PCR products of AthmiR167a. The diluted PCR products equal to 10, $10^2$, $10^3$, $10^4$, $10^5$, $10^6$, $10^7$ copy numbers of AthmiR167a. (D) Real-time PCR standard curve for AthmiR167a using diluted leaf cDNA as a template, which is equivalent to 1, 10, $10^2$, and $10^3$ ng total leaf RNA. (E) Relative level of PCR products using mismatched primer compare with perfectly matched primer in normal program (60°C annealing temperature) and high-stringency program (65°C annealing temperature) for amplifying the target AthmiR166a. (F) Mismatched positions in primer sequences and melting temperature ($T_m$) of these primers paired with the antisense oligonucleiotide of AthmiR166a.

for all tested miRNAs and 5.8S rRNA approached the maximum value (Table 2). Using AthmiR167a as an example, Figure 2C shows the standard curve derived from the amplification of various concentrations of AthmiR167a PCR products from leaf RNA and indicates that AthmiR167a quantities in the range of 10–$10^6$ copies can be reliably amplified with an efficiency nearing 2 (from the slope of -3.33). When using cDNA as the template transcribed from poly(A)-tailed total RNA, all tested miRNAs could be quantitatively amplified from 1 to 1000 pg total RNA with an efficiency of about 2 (e.g., as shown in Figure 2D for AthmiR167a). The analyses further revealed that for most cases, the template quantities corresponding to 10–100 pg total RNA would yield optimal amplification efficiency and specificity, suggesting that our real-time PCR approach would be particularly useful for quantifying low copy number or underexpressed miRNAs. For instance, using approximately 500 pg total RNA, our approach may allow a quantitative amplification of *Arabidopsis* miRNAs having only one copy per cell, based on the assumption that there is 20–50 pg total RNA per cell in *Arabidopsis* (24,25).

To further verify the specificity of our real-time PCR approach, we tested the amplification of AthmiR166a with primers having perfect or 1–3 nucleotide mismatched complementarity to AthmiR166a sequence (Table 1). Using the normal PCR program, two and three mismatched primers (Figure 2E, 166-2m and 166-3m) did not result in detectable amplification products, whereas AthmiR166a was quantitatively amplified using perfectly matched primer (Figure 2E, 60°C), demonstrating that such a PCR program can readily discern the expression of miRNAs from that of their paralogs differing by two or more nucleotides. However, all 1-nucleotide mismatched primers led to rather extensive product amplification. This was likely due to an efficient annealing of AthmiR166a and the 1-nucleotide mismatched primer (Figure 2E, 60°C). We therefore modified the annealing temperature for the PCR program by first determining experimentally the true $T_m$ values for these primers. To do that, antisense AthmiR166a sequence was used as the annealing fragment for all primers tested. The true $T_m$ values are listed in Figure 2F and based on these, we raised the PCR annealing temperature to 65°C, which is higher than the $T_m$s for all tested 1-nucleotide mismatched primers but still 5°C below the $T_m$ of the perfectly matched target AthmiR166a primer. As expected, the modified PCR amplification drastically reduced the nontarget amplification products to insignificant levels (Figure 2E, 65°C) and did not affect the amplification efficiency of AthmiR166a with its perfectly matched primer. Taken together, these results attested to an effective real-time PCR amplification system suitable for discerning miRNAs having as few as 1 nucleotide sequence difference.

The real-time PCR determined expression patterns of some of the

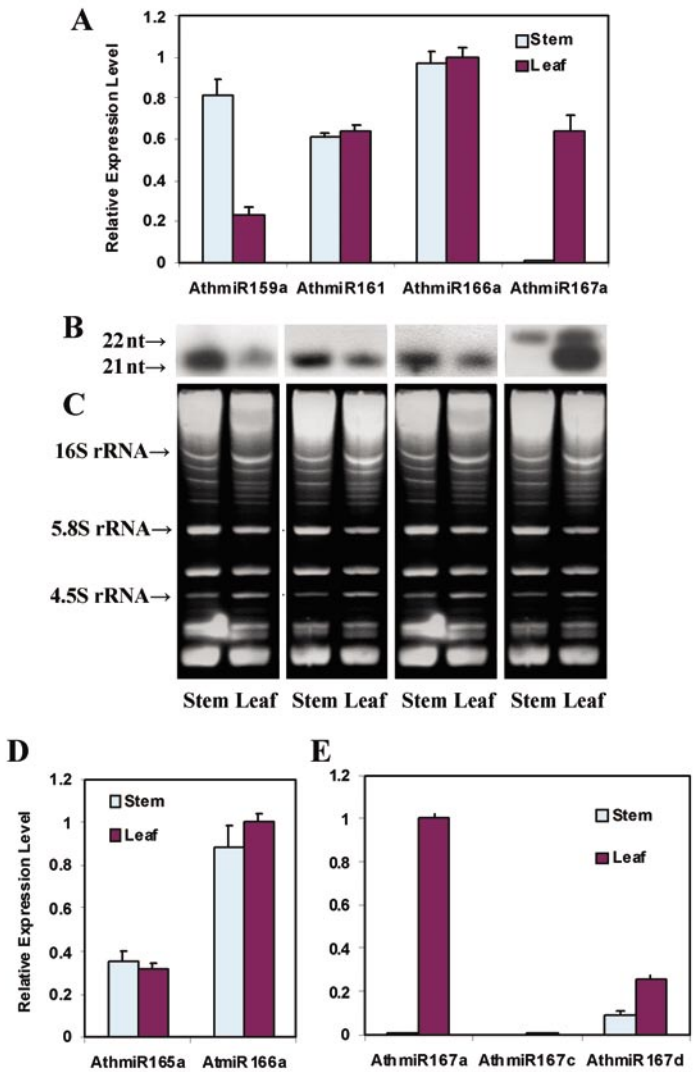


**Figure 3. The characterization of microRNA (miRNA) expression patterns by real-time PCR and Northern blot analysis.** (A) Relative expression levels of AthmiR159a, AthmiR161, AthmiR166a, and AthmiR167a in stem and leaf tissues by real-time PCR using cDNAs equivalent to 100 pg total RNA and normal PCR program. (B) Northern blot analysis of AthmiR159a, AthmiR161, AthmiR166a, and AthmiR167a expression using their antisense probes, respectively. Twenty micrograms total RNA/lane. (C) RNA separates on 12% polyacrylamide, 8 M urea gel as loading control. (D) Relative expression of AthmiR165a and AthmiR166a quantified by high-stringency PCR program. (E) Relative expression of AthmiR167a, AthmiR167c, and AthmiR167d using normal PCR program. The expression levels of all miRNAs by real-time PCR were relative to the expression of *Arabidopsis* 5.8S rRNA and normalized. nt, nucleotides.

target miRNAs in leaf and stem tissues (Figure 3A) were consistent with those by Northern blot analysis (Figure 3B). Northern blot analysis can be a useful method for detecting miRNAs having distinct sequences, such as AthmiR159a and AthmiR161. However, it cannot discriminate miRNAs with an identical size and with a high sequence homology that express in the same tissue. The Northern blot analysis signals seen in stem and leaf tissues for AthmiR166a could represent those of either AthmiR166a or AthmiR165a or both, since AthmiR165a and AtmiR166a are both 21 nucleotides but differ by 1 nucleotide in their sequences (3,18). In contrast, the expression of these miRNAs could readily be discriminated by our real-time PCR system (Figure 3D), using their miRNA-specific primers (Table 1) and the modified program (65°C annealing temperature). AthmiR166a is apparently a more prevalent type of miRNA in both stem and leaf tissues as compared with AthmiR165a—a distinction that cannot be resolved by Northern blot analysis (Figure 3D).

Based on the current miRNA database (18), there are four members in the AthmiR167 family: (*i*) AthmiR167a, with 21 nucleotides; (*ii*) AthmiR167b, with 21 nucleotides; (*iii*) AthmiR167c, with 21 nucleotides; and (*iv*) AthmiR167d, with 22 nucleotides. In fact, AthmiR167a and AthmiR167b represent the identical mature miRNA from two distinct miRNA precursors. AthmiR167a and AthmiR167c differ by 2 nucleotides, and AthmiR167a also has a 2-nucleotide difference to AthmiR167d. It was previously reported that the probe to AthmiR167a detected the accumulation of 21-nucleotide size transcripts in all *Arabidopsis* tissue examined, except in stem, where a 22-nucleotide RNA accumulates (3). Using the probe to AtmiR167a, we detected a very weak signal of the 21-nucleotide RNA stems but detected the 22-nucleotide RNA transcripts in stems as well as in leaves (Figure 3B, right panel), consistent with the previous report (3). However, the identity of this 22-nucleotide RNA was unknown, because either the 21-nucleotide AthmiR167a or the 22-nucleotide AthmiR167d probes would hybridize to the 21- and 22-nucleotide RNA transcripts on a Northern blot analysis, casting doubt also about the identity of the 21-nucleotide RNA transcripts (3). We then amplified these AthmiR167 members using our standard real-time PCR program and their specific primers (Table 1) and provided quantitative evidence that the 22-nucleotide bands seen in the Northern blot analysis are the transcripts of AthmiR167d (Figure 3B, right panel), and that its transcript level in leaves is about triple that in stems, which is consistent with the signal levels revealed by the Northern analysis (Figure 3B, right panel). The real-time PCR result on the AthmiR167a type (Figure 3E) also indicated that the high 21-nucleotide transcript level in leaves and its insignificant level in stems seen in the Northern blot analysis (Figure 3B, right panel) are likely those of the transcripts of the AthmiR167a type. Essentially, no AthmiR167c transcripts could be detected in these two tissue types (Figure 3E), further confirming that the strong 21-nucleotide signal seen in the Northern analysis was primarily from AthmiR167a.

## Conclusion

Here we report a real-time PCR protocol for quantifying plant miRNAs. This method is sensitive enough to quantify miRNAs having low copy numbers and a similar length but differ by as few as a single nucleotide sequence. This mature miRNA-specific quantitation can be a useful supplement to the previously established pre-miRNA-specific PCR system (17) for a more comprehensive characterization of miRNA processing and maturation associated with the functions of miRNAs.


## ACKNOWLEDGMENTS

*We thank Jeff Kimbrough for providing the* Arabidopsis *plants. We also thank Catherine Clark, Shanfa Lu, and Ying-Hsuan Sun for comments on the manuscript. This work was supported by a grant from the U.S. Department of Energy Division of Energy Biosciences DE-FG02-03ER15442 to V.L.C.*


## COMPETING INTERESTS STATEMENT

*The authors declare no competing interests.*

## REFERENCE


1. **Bartel, D.P.** 2004. MicroRNAs: genomics, biogenesis, mechanism, and function. Cell *116*:281-297.
2. **Ambros, V.** 2004. The functions of animal microRNAs. Nature *431*:350-355.
3. **Reinhart, B.J., E.G. Weinstein, M.W. Rhoades, B. Bartel, and D.P. Bartel.** 2002. MicroRNAs in plants. Genes Dev. *16*:1616-1626.
4. **Sunkar, R. and J.-K. Zhu.** 2004. Novel and stress-regulated microRNAs and other small RNAs from *Arabidopsis*. Plant Cell *16*:2001-2019.
5. **Jones-Rhoades, M.W. and D.P. Bartel.** 2004. Computational identification of plant microRNAs and their targets, including a stress-induced miRNA. Mol. Cell *14*:787-799.
6. **Berezikov, E., V. Guryev, J. van de Belt, E. Wienholds, R.H. Plasterk, and E. Cuppen.** 2005. Phylogenetic shadowing and computational identification of human microRNA genes. Cell *120*:21-24.
7. **Adai, A., C. Johnson, S. Mlotshwa, S. Archer-Evans, V. Manocha, V. Vance, and V. Sundaresan.** 2005. Computational prediction of miRNAs in *Arabidopsis thaliana*. Genome Res. *15*:78-91.
8. **Ohler, U., S. Yekta, L.P. Lim, D.P. Bartel, and C.B. Burge.** 2004. Patterns of flanking sequence conservation and a characteristic upstream motif for microRNA gene identification. RNA *10*:1309-1322.
9. **Allawi, H.T., J.E. Dahlberg, S. Olson, E. Lund, M. Olson, W.P. Ma, T. Takova, B.P. Neri, and V.I. Lyamichev.** 2004. Quantitation of microRNAs using a modified Invader assay. RNA *10*:1153-1161.
10. **Barad, O., E. Meiri, A. Avniel, R. Aharonov, A. Barzilai, I. Bentwich, U. Einav, S. Gilad, et al.** 2004. MicroRNA expression detected by oligonucleotide microarrays: system establishment and expression profiling in human tissues. Genome Res. *14*:2486-2494.
11. **Krichevsky, A.M., K.S. King, C.P. Donahue, K. Khrapko, and K.S. Kosik.** 2003. A microRNA array reveals extensive regulation of microRNAs during brain development. RNA *9*:1274-1281.
12. **Calin, G.A., C.G. Liu, C. Sevignani, M. Ferracin, N. Felli, C.D. Dumitru, M. Shimizu, A. Cimmino, et al.** 2004. MicroRNA profiling reveals distinct signatures in B cell chronic lymphocytic leukemias. Proc. Natl. Acad. Sci. USA *101*:11755-11760.
13. **Miska, E.A., E. Alvarez-Saavedra, M. Townsend, A. Yoshii, N. Sestanm, P. Rakicm, M. Constantine-Paton, and H.R. Horvitz.** 2004. Microarray analysis of microRNA expression in the developing mammalian brain. Genome Biol. *5*:R68.

14. **Babak, T., W. Zhang, Q. Morris, B.J. Blencowe, and T.R. Hughes.** 2004. Probing microRNAs with microarrays: tissue specificity and functional inference. RNA *10*:1813-1819.
15. **Baskerville, S. and D.P. Bartel.** 2005. Microarray profiling of microRNAs reveals frequent coexpression with neighboring miRNAs and host genes. RNA *11*:241-247.
16. **Liang, R.Q., W. Li, Y. Li, C.Y. Tan, J.K. Li, Y.X. Jin, and K.C. Ruan.** 2005. An oligonucleotide microarray for microRNA expression analysis based on labeling RNA with quantum dot and nanogold probe. Nucleic Acids Res. *33*:e17.
17. **Schmittgen, T.D., J. Jiang, Q. Liu, and L. Yang.** 2004. A high-throughput method to monitor the expression of microRNA precursors. Nucleic Acids Res. *32*:e43.
18. **Griffiths-Jones, S.** 2004. The microRNA Registry. Nucleic Acids Res. *32*:D109-D111.
19. **Lu, S., R. Shi, C.C. Tsao, X. Yi, L. Li, and V.L. Chiang.** 2004. RNA silencing in plants by the expression of siRNA duplexes. Nucleic Acids Res. *32*:e171.
20. **Park, W., J. Li, R. Song, J. Messing, and X. Chen.** 2002. CARPEL FACTORY, a Dicer homolog and HEN1, a novel protein, act in microRNA metabolism in *Arabidopsis thaliana.* Curr. Biol. *12*:1484-1495.
21. **Livak, K.J. and T.D. Schmittgen.** 2001. Analysis of relative gene expression data using real-time quantitative PCR and the $2^{-\Delta\Delta CT}$ Method. Methods *25*:402-408.
22. **Winer, J., C.K. Jung, I. Shackel, and P.M. Williams.** 1999. Development and validation of real-time quantitative reverse transcriptase-polymerase chain reaction for monitoring gene expression in *cardiac myocytes* in vitro. Anal. Biochem. *270*:41-49.
23. **Yehudai-Resheff, S. and G. Schuster.** 2000. Characterization of the *E. coli* poly(A) polymerase: nucleotide specificity, RNA-binding affinities and RNA structure dependence. Nucleic Acids Res. *28*:1139-1144.
24. **Wang, H.Y., R.L. Malek, A.E. Kwitek, A.S. Greene, T.V. Luu, B. Behbahani, B. Frank, J. Quackenbush, and N.H. Lee.** 2003. Assessing unmodified 70-mer oligonucleotide probe performance on glass-slide microarrays. Genome Biol. *4*:R5.
25. **Hilson, P., J. Allemeersch, T. Altmann, S. Aubourg, A. Avon, J. Beynon, R.P. Bhalerao, F. Bitton, et al.** 2004. Versatile gene-specific sequence tags for *Arabidopsis* functional genomics: transcript profiling and reverse genetics applications. Genome Res. *14*:2176-2189.

Received 31 March 2005; accepted 13 May 2005.

*Address correspondence to Vincent L. Chiang, Forest Biotechnology Group, Department of Forestry and Environmental Resources, Campus Box 7247, 2500 Partners II Bldg., 840 Main Campus Drive, North Carolina State University, Raleigh, NC 27695-7247, USA. e-mail: Vincent_Chiang@ncsu.edu*